Initiation and growth of thermal fatigue crack networks in a 304 L type steel

V. Maillot[1,2], A. Fissolo[1], G. Degallaix[2], S. Degallaix[2], B. Marini[1], J.-C. Le Roux[3]

[1] CEA-DEN Commissariat à l'Energie Atomique – Saclay, 91191 Gif sur Yvette Cedex, France
[2] Ecole Centrale de Lille – L.M.L. (URA CNRS 1441) – BP48, 59651 Villeneuve d'Ascq Cedex, France
[3] EDF-MMC Electricité de France – Centre des Renardières, 77818 Moret sur Loing Cedex, France

ABSTRACT: *Various components of nuclear reactors are submitted to very sharp thermo-mechanical loadings. Thermal fatigue cracking has been clearly detected in auxiliary loops of the primary cooling circuit of Pressurized Water Reactors (PWRs). The study presented here is focused on the 304 L type stainless steel used in PWRs. The thermal fatigue behavior of this steel has been investigated using a specific thermal fatigue facility called „SPLASH test equipment". This test equipment allows the reproduction of multiple cracking networks similar to those detected during in-service inspections. The present study deals with the three following points:*
i) the experimental determination of crack initiation conditions and the morphological description of the growing crack networks;
ii) the growth and shielding effect between cracks of the networks tested under four point bending fatigue crack growth conditions;
iii) the multiple crack growth numerical simulation, using Skelton's model, and a generalized Paris' law. In spite of simplified assumptions, this modelling, gives predictions in good agreement with observations, as far as the evolution of the mean and deepest cracks during cycling are concerned.

INTRODUCTION

Thermal fatigue induces in-service damage in numerous industrial components, such as moulds, rolling mill cylinders or turbine blades. Some examples are given by Bressers and Rémy [1] or Spera and Mowbray [2]. Such damage sometimes also occurs in different types of nuclear reactor components. In the case of Pressurized Water Reactors (PWRs), crack networks may appear in auxiliary loop zones, next to a cold water injection site, in spite of relatively small temperature fluctuations [3]. The present

study is focused on the crack networks obtained under PWR thermal conditions using the SPLASH facility as described in the first paragraph. In most networks, the crack depth remains small. The network parameters are described in the second paragraph. Nevertheless, some additional loading could occur in service, and propagate the cracks initiated under thermal fatigue. Bending is one of the possible additional loadings. The propagation mechanisms and the shielding effect of the cracks in the network are therefore investigated experimentally under cyclic four-point bending, and numerically using a crack propagation simulation, as reported respectively in the third and fourth paragraphs.

THE SPLASH EQUIPMENT

For in-service components, thermo-mechanical loadings usually come from temperature gradients in thickness. The SPLASH equipment was developed in order to reproduce such gradients on two opposite sides of a parallelepipedic specimen (240x30x20 mm^3). Figures 1 and 2 present respectively the testing facility and the specimen. The specimen is continuously heated by an electrical DC current (Joule effect), and cyclically submitted to thermal down-shocks (corresponding to a cooling rate of about 500 to 1000°C/s) when water is sprayed on opposite faces.

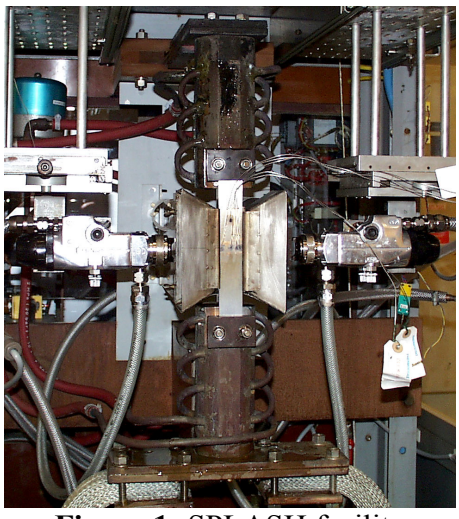

Figure 1: SPLASH facility

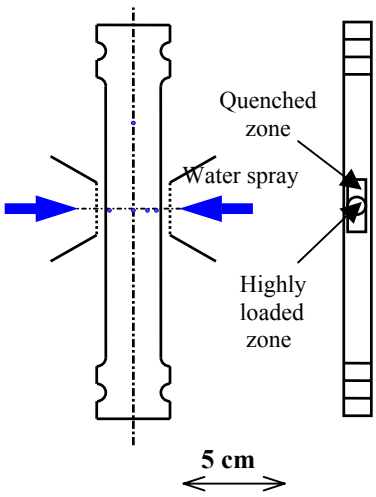

Figure 2: SPLASH specimen

Two types of specimens are used: calibration specimens and test specimens. Both are instrumented with four K-type thermocouples brazed in

depth, at 3 and 7 mm from the left and right surfaces. Calibration specimens carry two additional thermocouples brazed at the center of the left and right quenched surfaces, and are used to determine the parameters of the water spray necessary to obtain the selected temperature range ΔT at the surface. The test specimens are not equipped with those surface thermocouples, in order to avoid premature crack initiation.

The steel studied here is a 304 L type austenitic stainless steel. Its chemical composition is given in Table 1.

TABLE 1: Chemical composition of the 304 L type steel in wt%

C	Mn	Si	Cr	Ni	Mo	S	P	Cu	Al	B	N	Fe
0.031	1.48	0.55	19.4	8.6	0.23	0.003	0.028	0.17	0.025	0.0015	0.058	Bal

The thermal conditions of the tests are given in Table 2. Six specimens were tested: 2 with ΔT=200°C and 4 with ΔT=150°C, for different maximal numbers of cycles.

TABLE 2: Thermal test conditions

Maximum temperature	Temperature range	Maximal number of cycles
Tmax = 320°C	ΔT = 150 or 200°C	300,000 or 500,000

The number of cycles to initiation N_i is determined using regular observations of the quenched surfaces by optical microscopy, after the removal of the thin oxide layer that forms during cycling. For these observations, the tests are interrupted each 10,000 cycles. It is considered that initiation occurs when at least one crack with a length at the surface of 50 to 150 μm is observed.

After initiation, the growth and coalescence of the cracks, then the formation of a network are observed regularly during the test. Then the test is stopped at a chosen number of cycles. After the end of the test, the 3D character of the crack networks is examined, using a step-by-step removal of thin layers.

NETWORK PARAMETERS

In order to characterize the growth of the networks, various geometrical and statistical parameters can be determined on the surface of the specimen during the cycling, and in depth, at the end of the test.

Initiation

Initiation is observed at around 70,000 – 80,000 cycles for ΔT=150°C and at around 60,000 cycles for ΔT=200°C.

Evolution of the network parameters on the surface during cycling

It takes time for the first cracks to grow, coalesce and form a network on the surface of the specimen. In Figure 3, for instance, the same network is shown after 150,000 cycles and 300,000 cycles. It was usually thought that a stabilization of the network should occur but the studied parameters such as the total crack length, the network size (defined as the smallest convex polygon containing the network) show that there is no stabilization at 300,000 cycles. The non-stabilization is evidenced by Figures 4 and 5.

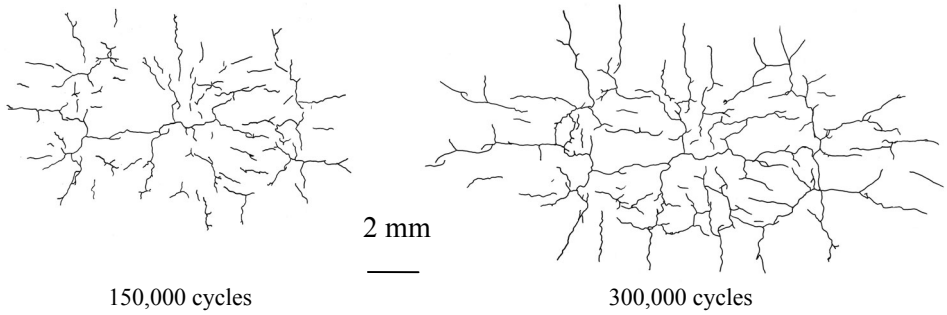

Figure 3: The same crack network, T_{max}=320°C, ΔT=200°C, observations at 150,000 and 300,000 cycles.

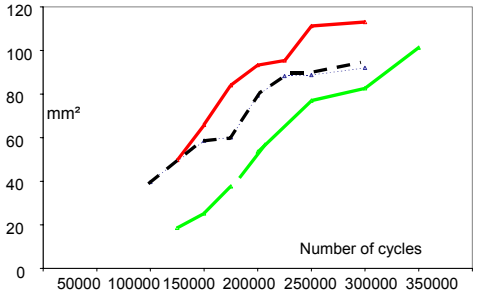

Figure 4: Networks area versus number of cycles for 3 different specimens, T_{max}=320°C, ΔT=150°C

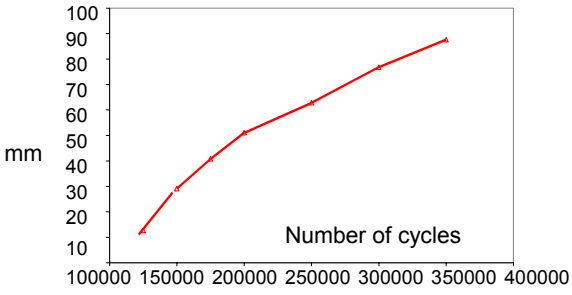

Figure 5: total crack length versus number of cycles, on the surface, T_{max}=320°C, ΔT=150°C

Network parameters in depth

Because of the sollicitation itself, there is a strong loading gradient in the specimen depth. Therefore, the cracks cannot propagate very deep. Furthermore, there is also a shielding effect, between neighbouring cracks, that slowed down and then stopped the propagation of the smaller ones.

Those foresighted effects appear clearly in the Figures 6 to 8. The total crack length strongly decreases after a few hundred micrometers, as most cracks stop, and the complexity of the network also diminishes as the depth increases, because only a few of the most important cracks still propagate.

The complexity of the network is expressed by the number of triple points, those points resulting from either the coalescence of two cracks or the branching of one crack into two.

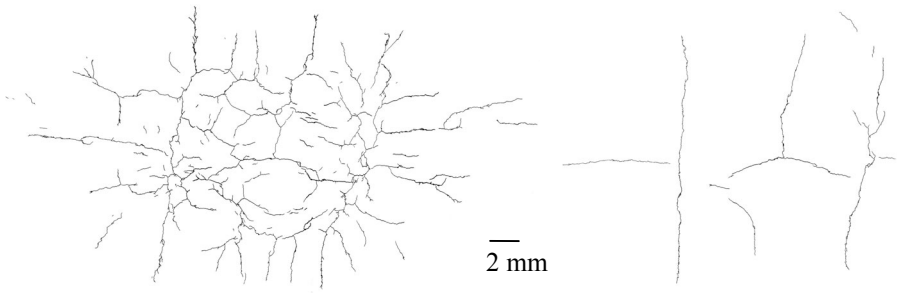

Figure 6: T_{max}=320°C, ΔT=200°C, 300,000 cycles; the same network at different depths

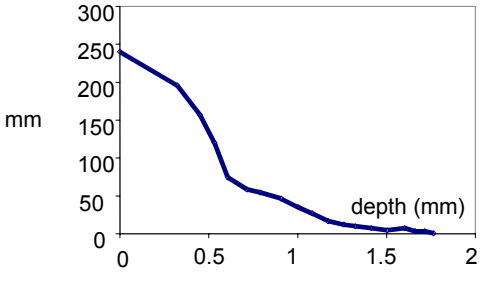

Figure 7: Evolution of the total crack length versus depth, T_{max}=320°C, ΔT=200°C, 150,000 cycles

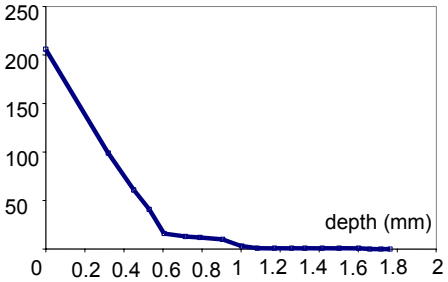

Figure 8: Number of triple points versus depth, T_{max}=320°C, ΔT=200°C, 150,000 cycles

CRACK NETWORK BEHAVIOUR UNDER CYCLIC FOUR-POINT BENDING

Some crack networks resulting from the SPLASH tests, were furthermore tested under isothermal cyclic four-point bending. The main purpose of those tests is to compare the propagation of a crack network with that of a single crack.

The tests are conducted under load control, at R = 0.1. The load range is the same throughout the test, and the stress intensity factor range, ΔK, grows as the crack length increases. There are two types of specimen. The first type carry a notch 1.5 mm deep (Figure 9), and in that case a single crack growth at notch tip. The second type bears a thermal fatigue crack network, and in that case at least one crack is deeper than 1.5 mm. Two notched specimens and three networks were tested.

For notched specimen, the crack length can be deduced from the evolution of the potential drop, using Johnson's formula as [4]. It is more difficult to evaluate the size of the network's cracks. The crack growth was followed with a video camera. Unfortunately, all the cracks of the network were not coming out on the specimen size. The Figure 10 compares the crack growth of a sigle crack and of four cracks from the same network (T_{max}=320°C, ΔT=150°C, 300,000 cycles) during the test.

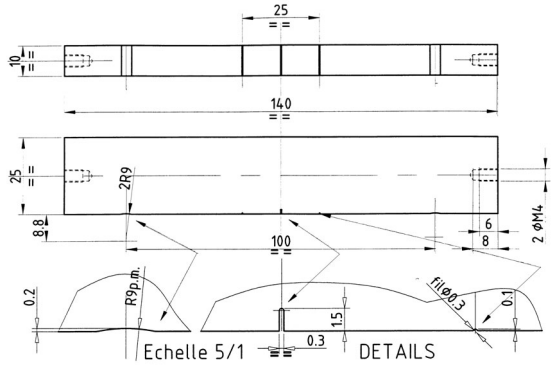

Figure 9: Geometry of a notched speciment for 4-point bending test

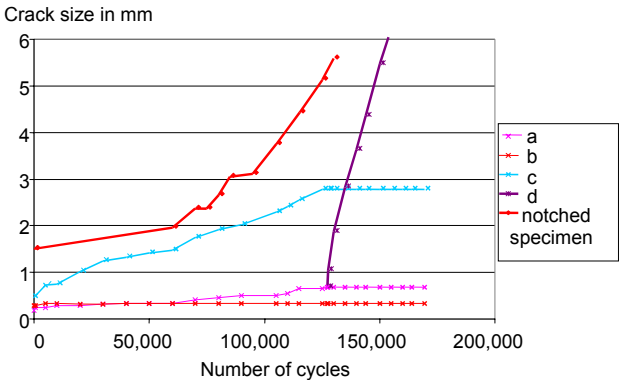

Figure 10: Growth of a single crack compared to the evolution of the 4 main cracks of a network under the same 4-point bending conditions

The results presented in Figure 10 first show that the single crack propagates more quickly than the different cracks of the network. In this particular case, the major crack (D) was not thorough at the begining of the test, and therefore not visible by the camera, but it was 2.4 mm deep at the center of the specimen.The smaller cracks A, B and C propagate then stop. B stopped quickly, entirely shielded almost immediately by its neighbour A. A had a significantly longer growth but was also stopped after 12,000 cycles when C started to be the dominant crack but it was finally shielded by D.

This test is only an example, but it very efficiently evidences the shielding effect mechanism. It also indicates that modelling a network by its deepest crack, similar to the single crack at the notched speciment tip, leads to an over-estimation of the crack growth.

An attempt to model the multiple crack growth by taking into account this shielding effect mechanism is presented in the next paragraph.

SIMULATION

The 2D modelling was designed to account for the propagation under thermal loading, in depth, of multiple parallel cracks. The propagation of an isolated crack was firstly investigated, then that of two cracks, and finally, that of up to ten cracks [6]. The crack initiation is simulated first, and then the propagation.

Initiation

The simulation of crack initiation was performed in two steps. In the first step, a Monte Carlo randomization method is used to determine the size of

the surface grains, according to a distribution law of the experimentally measured grain sizes. The obtained grains are square-shaped. In the second step, another Monte Carlo randomization gives to each grain a position relative to the surface.

In the present development of the modelling, it is assumed that right from the beginning, each grain is completely cracked in its middle. This assumption is an oversimplification: it was observed experimentally that only one out of four or five grains is cracked and that the cracks do not appear at the same time.

After this initiation hypothesis, the simulation of crack growth can be performed.

Propagation

The thermo-mechanical loadings are first calculated. Near the surface, the stresses are equibiaxial. A Skelton's law [7] is used to define an equivalent stress intensity factor. According to Eq. 1, the strain loading can be reduced to an elastic stress loading which follows the Linear Elastic Fracture Mechanics laws:

$$\Delta\sigma_{eff} = q\Delta\sigma + \Delta\sigma_{pseudo} \quad \text{and} \quad \Delta\sigma_{pseudo} = \frac{E\Delta\varepsilon_p}{(1-\nu)} \tag{1}$$

$q\Delta\sigma$ represents the part of the cycle when the crack is open, whereas $\Delta\sigma_{pseudo}$ takes into account the plasticity at the crack tip. For the present purpose, q was estimated to be close to 0.6.

$\Delta\sigma_{eff}$ is fitted with a third degree polynomial as presented in Eq. 2:

$$\Delta\sigma_{eff}(x) = \sum_{i=0}^{i=3} A^i\left(x^i\right) \tag{2}$$

ΔK_{eff} is then calculated using the superposition method of Buchalet and Bamford [7], as presented in Eq.3. for a crack of depth a:

$$\Delta K_{eff}(a) = \sqrt{\pi a}\left[A_0F_1 + \frac{2a}{\pi}A_1F_2 + \frac{a^2}{2}A_2F_3 + \frac{4a^3}{3\pi}A_3F_4\right] \tag{3}$$

where F_1, F_2, F_3 and F_4 depend on the geometry, and particularly on the other cracks (depths and distances from the studied crack). The values of the F_i are tabulated, in order to make the calculations faster. The growth of each crack then follows a generalized Paris' law, as presented in Eq. 4, for a given number of cycles increment (usually, dN = 500).

$$\frac{da}{dN} = C\left(\Delta K_{eff}\right)^m \tag{4}$$

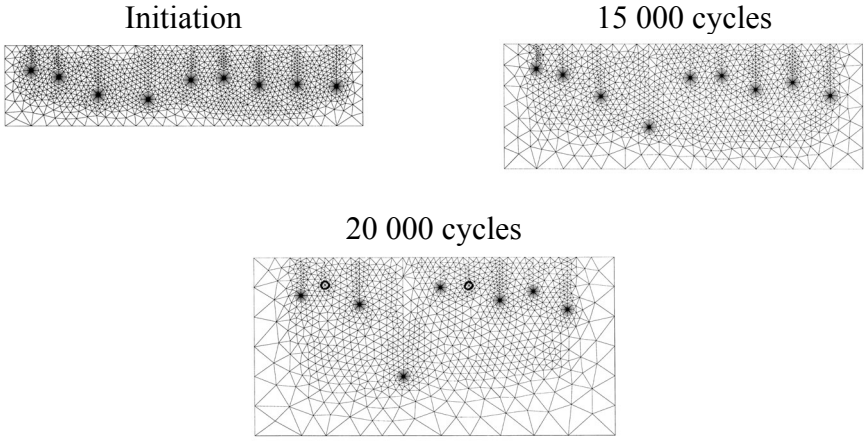

Figure 11: Example of propagation of a 10-crack network

This simulation emphasizes the mutual shielding of neighboring cracks: a smaller crack next to a deeper will slow down the growth of the deeper, whereas its own growth will be slowed even more. Eventually, the smaller crack stops growing altogether.

In the future, it is planned to introduce some modifications to the model to make it really efficient: a progressive crack initiation could be a first step.

CONCLUSION

The thermal fatigue equipment SPLASH can reproduce multiple cracking networks with characteristics similar to those observed on in-service components. Cyclic four-point bending tests on the obtained thermal fatigue networks proves the importance of the mutual shielding effect of neigbouring cracks.

The 2D simulation of crack growth in depth gives satisfying results as far as the shielding effect, the maximum and the average crack depth are concerned, but still need further work to be really efficient.

REFERENCES

1. Bressers, J. Rémy, L. 1996 Fatigue under Thermal and Mechanical Loading, Kluwer Acad. Pub.

2. Spera D.A., Mowbray D.F., 1976 Thermal fatigue of materials and components *ASTM STP 612.*
3. de Keroulas F., Thomeret B., 1990 *Société Française d'Energie Nucléaire* Vol. 1, pp. 107-117.
4. Amzallag, C. et al., 1991 Pratique des essais de propagation de fissure en fatigue, *AFNOR*, A 03-404.
5. Fissolo A., Marini B., Nais G., Wident P ., 1996 Thermal Fatigue behaviour for a 316 L type steel, *Journal of Nuclear Materials,* 233-237, pp.156-161.
6. Fissolo A., Robertson C., Maillot V., Marini B. 2000 Prediction of cracking under thermal fatigue, *Proceedings of ECF 13, San Sebastian, Spain, 6-9 September 2000*.
7. Skelton R.P., 1983 Crack initiation and growth in simple metal components during thermal cycling, *Fatigue at high Temperature,* pp. 1-61.
8. Buchalet C.B., Bamford W.H., 1976 Mechanics of crack growth, *ASTM STP 590,* pp. 385-402.